A cationic fluorescent polymeric thermometer for the ratiometric sensing of intracellular temperature

Seiichi Uchiyama,*[a] Toshikazu Tsuji,*[a,b] Kumiko Ikado,[b] Aruto Yoshida,[b] Kyoko Kawamoto,[a] Teruyuki Hayashi[c] and Noriko Inada[c]

We developed new cationic fluorescent polymeric thermometers containing both benzothiadiazole and BODIPY units as an environment-sensitive fluorophore and as a reference fluorophore, respectively. The temperature-dependent fluorescence spectra of the thermometers enabled us to perform highly sensitive and practical ratiometric temperature sensing inside living mammalian cells. Intracellular temperatures of non-adherent MOLT-4 (human acute lymphoblastic leukaemia) and adherent HEK293T (human embryonic kidney) cells could be monitored with high temperature resolutions (0.01–1.0 °C) using the new cationic fluorescent polymeric thermometer.

[a]*Graduate School of Pharmaceutical Sciences, The University of Tokyo, 7-3-1 Hongo, Bunkyo-ku, Tokyo 113-0033, Japan. E-mail: seiichi@mol.f.u-tokyo.ac.jp*
[b]*Central Laboratories for Key Technologies, KIRIN Company Limited, 1-13-5 Fukuura, Kanazawa-ku, Yokohama-shi, Kanagawa 236-0004, Japan. E-mail: Toshikazu_2_Tsuji@kirin.co.jp*
[c]*Graduate School of Biological Sciences, Nara Institute of Science and Technology, 8916-5 Takayama-cho, Ikoma-shi, Nara 630-0192, Japan*

Introduction

Intracellular temperature has received widespread attention because it is assumed to be related to many cellular activities and the health status of cells.[1] Fluorescent thermometers[2] are promising analytical tools for intracellular thermometry[3–17] because of their high temperature resolution (better than 1 °C) and high spatial resolution (molecular scale in principle). In a previous study, we developed a fluorescent polymeric thermometer by combining a thermosensitive polymer with an environment-sensitive fluorophore, and we performed intracellular temperature mapping of mammalian cells using fluorescence lifetime imaging microscopy.[3] Recently, a cationic fluorescent polymeric thermometer with the ability to enter living cells was also developed for intracellular temperature measurements in yeast and mammalian cells.[4a] In these studies, the fluorescence lifetime was used as the temperature-dependent parameter, because it is insusceptible to fluctuations under the experimental conditions, such as the concentration of the fluorescent thermometer and the power of the excitation source. Here, we report a novel cationic fluorescent polymeric thermometer for the ratiometric sensing of intracellular temperature. In contrast to our previous thermometers, the fluorescence ratio at two different wavelengths is used as the temperature-dependent measurable parameter. The fluorescence ratio is another parameter that is mostly insusceptible to fluctuations under the experimental conditions.[18]

The chemical components of the novel cationic fluorescent polymeric thermometers are shown in Fig. 1a. The polymeric thermometers are random copolymers composed of the following four distinct units: (i) a thermosensitive NNPAM unit, which adopts an extended structure at low temperatures but shrinks to a globular structure at high temperatures; (ii) a cationic APTMA unit, which enables the spontaneous introduction of the thermometer into cells[4a] and prevents the intermolecular aggregation of the thermometer;[19] (iii) a fluorescent DBThD-AA unit,[20] which senses the change in the hydrophobicity/hydrophilicity as a result of the structural change in the NNPAM units and, consequently, produces a temperature-dependent fluorescence; and (iv) a fluorescent BODIPY-AA unit, which emits constant fluorescence as a reference signal. The fluorescence characteristics of BODIPY-AA units were estimated from those of pyrromethene 546 (Fig. 1b) reported in the literature.[21]

In this article, the novel synthesis of a fluorescent monomer BODIPY-AA and a model fluorescent compound BODIPY-IA (Fig. 1c) is described. The novelty of the fluorescent polymeric thermometers in this study lies in the use of two fluorophores (*i.e.*, DBThD-AA and BODIPY-AA units). The DBThD-AA units exhibit environment-sensitive fluorescence, whereas the BODIPY-AA units do not. To confirm this characteristic, the photophysical properties of the model compounds DBThD-IA[22] and BODIPY-IA are investigated. Three fluorescent

(a)

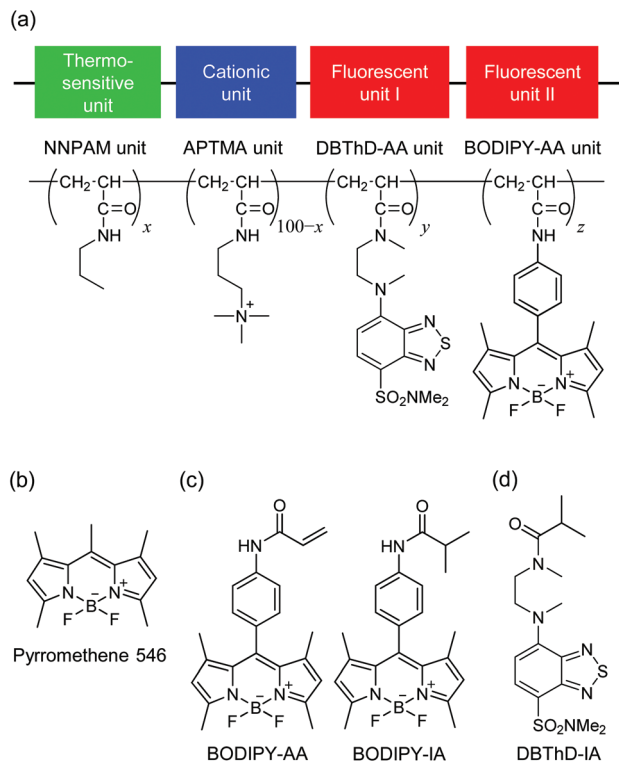(b)   (c)   (d)

Fig. 1 Chemical structures of (a) cationic fluorescent polymeric ther-mometers, (b) pyrromethene 546, (c) BODIPY-AA and BODIPY-IA, and (d) DBThD-IA. NNPAM, N-n-propylacrylamide; APTMA, (3-acrylamido-propyl)trimethylammonium; DBThD-AA, N-(2-{[7-(N,N-dimethyl-aminosulfonyl)-2,1,3-benzothiadiazol-4-yl]-(methyl)amino}ethyl)-N-methylacrylamide; BODIPY-AA, 8-(4-acrylamidophenyl)-4,4-difluoro-1,3,5,7-tetramethyl-4-bora-3a,4a-diaza-s-indacene; pyrromethene 546, 4,4-difluoro-1,3,5,7,8-pentamethyl-4-bora-3a,4a-diaza-s-indacene; BODIPY-IA, 4,4-difluoro-8-(4-isobutylamidophenyl)-1,3,5,7-tetramethyl-4-bora-3a,4a-diaza-s-indacene; DBThD-IA, N,2-dimethyl-N-(2-{methyl[7-(dimethylsulfamoyl)-2,1,3-benzothiadiazole-4-yl]amino}-ethyl)propanamide.

polymeric thermometers with different unit compositions are prepared, and their sensitivity to temperature variation is evaluated in an aqueous solution. The most sensitive fluorescent thermometer is applied to intracellular thermometry of non-adherent MOLT-4 (human acute lymphoblastic leukaemia) cells[23] and adherent HEK293T (human embryonic kidney) cells.[24] The function of the thermometer is demonstrated in biological experiments using the mammalian MOLT-4 and HEK293T cells to assess the sensitivity to temperature variation inside the cells as well as the incorporation efficiency and effects on cell viability.

Experimental

Materials and apparatus

NNPAM was synthesized and purified according to the general procedure for N-alkylacrylamides.[25] α,α′-Azobisisobutyronitrile (AIBN) was purchased from Wako Pure Chemicals and was

recrystallized from methanol. Acryloyl chloride and APTMA chloride were purchased from TCI. Water was purified using a Millipore Milli-Q system. All other reagents were guaranteed to be reagent grade and were used without further purification.

^{1}H NMR spectra were obtained by using a Bruker Avance 400 spectrometer. J values are given in hertz. Mass spectra acquired with an electrospray ionization (ESI) system were recorded with a Bruker micrOTOF-05 spectrometer. The melting points were measured with a Round Science RFS-10 and are uncorrected.

Synthesis

BODIPY-AA. 8-(4-Aminophenyl)-4,4-difluoro-1,3,5,7-tetra-methyl-4-bora-3a,4a-diaza-s-indacene (10 mg, 29 μmol)[26] was dissolved in acetonitrile (2 mL). After the addition of triethyl-amine (2.9 mg, 4.1 μL, 29 μmol) and acryloyl chloride (3.5 mg, 3.1 μL, 38 μmol) at 0 °C, the mixture was stirred at room tem-perature for 2 h. K_2CO_3 (40 mg) was then added to the reaction mixture, and after filtration, the mixture was evaporated to dryness under reduced pressure. The residue was purified by column chromatography on silica gel using dichloromethane–n-hexane (3 : 1 → 1 : 0) as the eluent to afford BODIPY-AA (11.1 mg, 97%) as an orange powder. Mp, 245–249 °C; ^{1}H NMR (400 MHz, methanol-d_4) δ 7.87 (2H, d, J 8.6), 7.30 (2H, d, J 8.6), 6.42–6.46 (2H, m), 6.07 (2H, s), 5.81 (1H, d, J 9.6), 2.49 (6H, s), 1.48 (6H, s); ^{13}C NMR (100 MHz, CDCl₃) δ 163.5, 155.5, 143.1, 141.1, 138.6, 131.6, 130.8, 128.8, 128.5, 121.2, 120.1, 14.6; HRMS (ESI): m/z calcd for $C_{22}H_{23}BF_2N_3O$ ([M + H]⁺): 394.1897. Found: 394.1900.

BODIPY-IA. 8-(4-Aminophenyl)-4,4-difluoro-1,3,5,7-tetra-methyl-4-bora-3a,4a-diaza-s-indacene (10 mg, 29 μmol)[26] was dissolved in acetonitrile (2 mL). After the addition of triethyl-amine (3.6 mg, 4.9 μL, 35 μmol) and isobutyric anhydride (7.0 mg, 7.4 μL, 44 μmol) at 0 °C, the mixture was stirred at 50 °C for 5 h. Na_2CO_3 (40 mg) was then added to the reaction mixture, and after filtration, the resulting mixture was evapo-rated to dryness under reduced pressure. The residue was purified by column chromatography on silica gel using dichloromethane as the eluent to afford BODIPY-IA (11.5 mg, 95%) as an orange powder. Mp, 252–254 °C (decomp); ^{1}H NMR (400 MHz, CDCl₃) δ 7.69 (2H, d, J 8.6), 7.31 (1H, br), 7.22 (2H, d, J 8.4), 5.98 (2H, s), 2.55 (6H, s), 1.59 (1H, s), 1.43 (6H, s), 1.29 (6H, d, J 6.8); ^{13}C NMR (100 MHz, CDCl₃) δ 175.3, 155.5, 143.1, 141.3, 138.9, 131.6, 130.5, 128.8, 121.2, 119.9, 36.9, 19.6, 14.6; HRMS (ESI): m/z calcd for $C_{23}H_{26}BF_2N_3NaO$ ([M + Na]⁺): 432.2029. Found: 432.2035.

Fluorescent polymeric thermometers. NNPAM (4.8 mmol), APTMA (0.2 mmol), DBThD-AA (25 μmol),[20] BODIPY-AA (5 μmol) and AIBN (50 μmol) were dissolved in N,N-dimethyl-formamide (10 mL), and the solution was bubbled with dry Ar for 30 min to remove dissolved oxygen. The solution was heated at 60 °C for at least 4 h and then cooled to room tem-perature. The reaction mixture was then poured into diethyl ether (300 mL). The resulting copolymer was collected by fil-tration and purified by dialysis. The contents of NNPAM and APTMA units in the copolymer were determined from the [1]H

Table 1 Physical properties of the fluorescent polymeric thermometers prepared in this study

Thermometer	Monomer ratio in feed[a]	Yield/%	Composition in thermometer $(x:y:z)$[b]	M_w[c]	M_n[d]	M_w/M_n	Sensitivity/% °C$^{-1,e}$
1	96 : 4 : 0.5 : 0.1	42	94.5 : 0.58 : 0.071	20 300	10 800	1.88	4.1
2	96 : 4 : 1 : 0.2	34	93.1 : 1.2 : 0.18	18 600	10 100	1.84	2.9
3	96 : 4 : 1.5 : 0.3	25	94.4 : 1.8 : 0.36	22 300	11 400	1.96	2.3

[a] NNPAM : APTMA : DBThD-AA : BODIPY-AA. [b] x, y and z indicate the composition of thermometers. See Fig. 1. [c] Weight-average molecular weight. [d] Number-average molecular weight. [e] Averaged change rate in the fluorescence ratio between 25 and 45 °C in 150 mM KCl solution.

NMR spectra (Bruker Avance 400). The proportions of the DBThD-AA and BODIPY-AA units in the copolymer were determined from the absorbance in methanol compared with the model fluorophores DBThD-IA[22] ($\varepsilon = 7900$ M^{-1} cm^{-1} at 447 nm and $\varepsilon = 1600$ M^{-1} cm^{-1} at 498 nm) and BODIPY-IA ($\varepsilon = 4800$ M^{-1} cm^{-1} at 447 nm and $\varepsilon = 83\,000$ M^{-1} cm^{-1} at 498 nm). The weight-average molecular weight (M_w) and number-average molecular weight (M_n) of the copolymer were determined by gel-permeation chromatography (GPC). The GPC equipment consisted of a JASCO PU-2080 pump, a JASCO RI-2031 refractive index detector, a JASCO CO-2060 column thermostat, and a Shodex GPC KD806-M column. A calibration curve was obtained using polystyrene standards, and 1-methyl-2-pyrrolidinone containing LiBr (5 mM) was used as the eluent. The reaction yields, actual compositions, and molecular weights are shown in Table 1.

Photophysical studies of BODIPY-IA

UV/Vis absorption spectra (30 μM) were recorded at 25 °C using a JASCO V-550 UV/Vis spectrometer. Fluorescence spectra (100 nM) were recorded at 25 °C with a JASCO FP-6500 spectrofluorimeter with a Hamamatsu R7029 optional photomultiplier tube (operating range, 200–850 nm). The fluorescence quantum yields (Φ_f) were determined from eqn (1) using a JASCO FP-8500 spectrofluorometer with a Hamamatsu R928 optional photomultiplier tube (operating range, 200–850 nm) and a JASCO ILF-835 integrating sphere unit,[27] in which the fluorescence spectra were corrected using a JASCO ESC-333 substandard light source (tungsten, 20 W):

$$\Phi_f = S_f/(S_{ex} - S_{ex'}) \tag{1}$$

where S_f is the area under the corrected fluorescence spectrum of a BODIPY-IA solution obtained with excitation at 458 nm, S_{ex} is the area under the corrected spectrum of the excitation light through a solvent and $S_{ex'}$ is the area under the corrected spectrum of unabsorbed excitation light that passes through a BODIPY-IA solution.

Measurements of the fluorescence spectra of the thermometers in KCl solutions

The fluorescence spectra of the synthesized fluorescent thermometers were recorded in KCl solutions at various temperatures using a JASCO FP-6500 spectrofluorometer. The sample temperature was controlled using a JASCO ETC-273 T temperature controller.

Introduction of the fluorescent thermometer 1 into MOLT-4 and HEK293T cells

Non-adherent MOLT-4 cells[23] were cultured at 37 °C with 5% CO$_2$ in RPMI (Roswell Park Memorial Institute) 1640 medium supplemented with 10% foetal bovine serum (FBS, Gibco). The cells were collected using centrifugation at 400g for 3 min and washed with 1 mL of a 5% glucose solution. After centrifugation at 400g for 3 min, the cells were resuspended in a 5% glucose solution at a density of 1×10^6 cells per mL. Then, thermometer 1 in water (5 w/v%, stored in a refrigerator or a freezer to prevent decomposition) was added to a 100-fold volume of cell suspension. The cells treated with the thermometer were incubated at 25 °C for 10 min,[4a] washed with 1 mL of PBS, collected using centrifugation at 400g for 3 min and resuspended in PBS. The incorporation of the thermometer into the HEK293T cells was performed without detaching cells. The HEK293T cells were cultured on a poly-L-lysine-coated 35 mm glass-bottom dish (Matsunami Glass Ind.) at 37 °C with 5% CO$_2$ in Dulbecco's modified Eagle's medium (DMEM, Gibco) supplemented with 5% FBS and 1% penicillin/streptomycin (Gibco). After the medium was removed, the cells were washed with a 5% glucose solution and then treated with a 5% glucose solution containing 0.05 w/v% of the thermometer. After incubation at 25 °C for 10 min, the cells were washed with PBS. A phenol red-free culture medium (Gibco) was used for live-cell imaging.

Flow cytometry

The fluorescence intensity of thermometer 1 in the MOLT-4 cells was measured using a flow cytometer (FACSCalibur, Becton Dickinson) with excitation at 488 nm and FL1 band-pass emission (530 ± 15 nm). Approximately 10 000 cells were analysed in each histogram.

Measurements of the fluorescence spectra of the fluorescent thermometer 1 in MOLT-4 cells

The fluorescence spectra of thermometer 1 in MOLT-4 cells were recorded at various temperatures using a JASCO FP-6500 spectrofluorometer. The cells treated with the thermometer were suspended in PBS in a cuvette (4 mL), and the cell suspension was stirred with a micro round magnetic stir bar

(diameter: 2 mm; stirring speed: 800 rpm). The sample temperature was controlled using a JASCO ETC-273 T temperature controller. The temperature resolution (δT) of **1** was evaluated using the following equation:[28]

$$\delta T = \left(\frac{\partial T}{\partial F_{\text{ratio}}}\right)\delta F_{\text{ratio}} \tag{2}$$

where $\partial T/\partial F_{\text{ratio}}$ and δF_{ratio} represent the inverse of the slope of the fluorescence ratio–temperature diagram and the SD of the fluorescence ratio, respectively. The SD value was obtained by triplicate measurements of one sample at each temperature.

Fluorescence imaging of MOLT-4 and HEK293T cells

MOLT-4 and HEK293T cells treated with thermometer **1** were observed using a confocal microscope (FV1000, Olympus) with a UPLS APO 100× lens (Olympus, N.A. 1.4) and UPlan 60× lens (Olympus, N.A. 1.35). The emission from the thermometer between 500 and 600 nm was collected under excitation at 473 nm. For the fluorescence imaging of MOLT-4 cells, approximately 10 μL of the cell suspension was dropped onto a coverslip and observed immediately. HEK293T cells were directly imaged in the glass-bottom dish. To measure the fluorescence spectra of thermometer **1** in the HEK293T cells using a confocal microscope, the excitation light was delivered to the sample *via* an 80/20 reflector. Spectral scans were acquired from 490 to 740 nm (10 nm step) with 10 nm wide bins. The resulting fluorescence images were analysed using FluoView (Olympus). The fluorescence intensity at each wavelength was obtained from the fluorescence images by summing and averaging the fluorescence intensities at all pixels within a single HEK293T cell. The temperature of the culture medium was controlled with a microscope cage incubation chamber (Water Jacket Top Stage Incubator H101, Oko-Lab). The incorporation efficiencies (%) were determined using eqn (3):

$$\text{Incorporation efficiency (\%)} = \text{number of cells containing the thermometer/number of cells} \times 100 \tag{3}$$

The total cell number was approximately 100, and the cells showing a fluorescence intensity higher than the threshold (maximum autofluorescence intensity) were counted as the cells containing the thermometer. The temperature resolution in intracellular thermometry of HEK293T cells was evaluated using the averaged fluorescence ratios of **1** in a HEK293T cell extract (0.01 w/v%). The HEK293T cell extract was prepared using a previously described procedure.[3]

Viability assay

The propidium iodide (PI, Sigma) assay was used to determine the cell viability. In the assay for the MOLT-4 cells, 15 μL of a PI solution (2 μg mL^{-1} in PBS) was mixed with 30 μL of the suspension of cells treated with thermometer **1**. In the HEK293T cell assay, 0.5 mL of the PI solution (2 μg mL^{-1} in PBS) was added to the cells treated with thermometer **1** and

Hoechst 33342 in 1 mL of DMEM medium.[29] Hoechst 33342 was used for the identification of each cell. Both cell lines were incubated with PI at 37 °C for 30 min. Fluorescence images of PI were acquired *via* excitation at 559 nm by recording the emission between 655 and 755 nm using the variable band-pass filter sets of a DM405/473/559 excitation dichroic mirror. The cell viabilities (%) were determined using eqn (4):

$$\text{Cell viability (\%)} = \text{number of PI negative cells/number of cells containing thermometer } \mathbf{1} \times 100 \tag{4}$$

Cell synchronization

The MOLT-4 cells were synchronized using the previously described double thymidine block method.[30] The cells were cultured in RPMI 1640 medium containing 2 mM thymidine (Wako Chemical) for 12 h. The cells were collected using centrifugation at 400g for 3 min, washed with PBS and then cultured for an additional 12 h in the thymidine-free medium. They were treated with the medium containing 2 mM of thymidine again for 12 h. The cells were then washed twice and resuspended in the thymidine-free medium.

Results and discussion

Fluorescence properties of DBThD-IA and BODIPY-IA

Representative absorption and fluorescence spectra of DBThD-IA and BODIPY-IA are shown in Fig. 2, and the photophysical data in 5 solvents with various polarities and hydrogen-bonding abilities (*i.e.*, *n*-hexane, ethyl acetate, acetonitrile, methanol and a mixture of water and 1,4-dioxane (3:1, v/v)) are summarized in Table 2. As described in detail in our previous paper,[20] the fluorescence properties of DBThD-IA were influenced by both the polarity of the environment and hydrogen bonding with solvent molecules. DBThD-IA emitted a stronger fluorescence signal at a shorter wavelength in apolar and aprotic solvents. In contrast, the fluorescence properties of BODIPY-IA were relatively insensitive to its environment. BODIPY-IA showed almost identical fluorescence characteristics in the 5 solvents tested in this study. These differences in the fluorescence properties of DBThD-IA and BODIPY-IA made them suitable as the fluorophores in polymeric thermometers because they can produce a temperature-dependent fluorescence ratio. In addition, the absorption and fluorescence spectra (shown in Fig. 2) suggested that a fluorescence ratio of polymeric thermometers at two different emission wavelengths could be obtained by excitation at a single wavelength because DBThD-IA and BODIPY-IA have overlapping absorption bands (*ca.* 450–500 nm) and distinctly separated emission maxima (*ca.* 510–515 nm and 560–585 nm, respectively), which is another advantage of the combination of these fluorophores in polymeric thermometers.
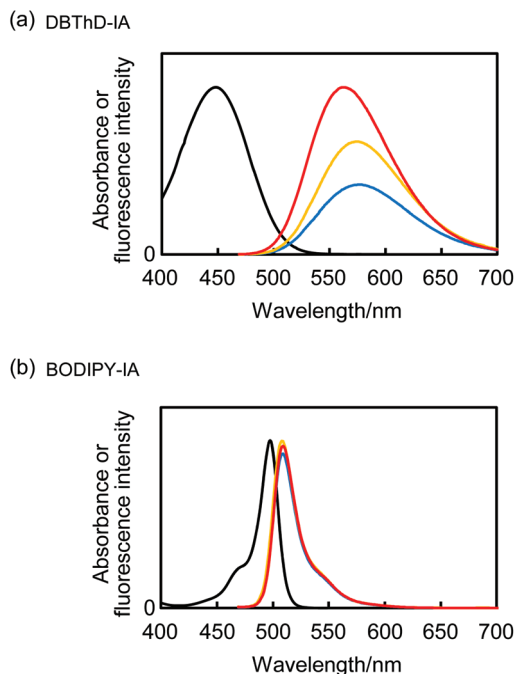
(a) DBThD-IA

(b) BODIPY-IA

Fig. 2 Representative absorption and fluorescence spectra of DBThD-IA and BODIPY-IA. The absorption spectra (30 μM for DBThD-IA and BODIPY-IA) were measured in acetonitrile (black). The fluorescence spectra (1 μM for DBThD-IA; 100 nM for BODIPY-IA) were measured with excitation at 458 nm in ethyl acetate (red), acetonitrile (orange) and methanol (blue).

Table 2 Photophysical properties of DBThD-IA and BODIPY-IA at 25 °C: maximum absorption wavelength (λ_{abs}), molar absorption coefficients (ε), maximum emission wavelength (λ_{em}) and fluorescence quantum yield (Φ_f)

Compound	Solvent	λ_{abs}/ nm	ε/M^{-1} cm^{-1}	λ_{em}/ nm	Φ_f
DBThD-IA[a]	n-Hexane	449	8100	529	0.81
	Ethyl acetate	449	7600	563	0.68
	Acetonitrile	448	8000	574	0.49
	Methanol	447	7900	575	0.27
	Water–1,4-dioxane (3 : 1, v/v)	450	8100	595	0.089
BODIPY-IA	n-Hexane	502	86 000	512	0.35
	Ethyl acetate	499	86 000	509	0.43
	Acetonitrile	497	83 000	508	0.38
	Methanol	498	83 000	509	0.39
	Water–1,4-dioxane (3 : 1, v/v)	500	81 000	512	0.53

[a] From ref. 20.

Preparation of cationic fluorescent polymeric thermometers 1–3 and their fluorescence responses to temperature variation in 150 mM KCl solution

Cationic fluorescent polymeric thermometers **1–3** were prepared *via* random copolymerisation. In the reaction feed, the molar ratio of NNPAM and APTMA was fixed at 96 : 4 based on

our previous polymeric thermometers.[4b] The molar ratio of DBThD-AA and BODIPY-AA was also fixed at 5 : 1 based on the fact that the molar absorption coefficient of DBThD-IA is smaller than that of BODIPY-IA (see Table 2). The physical properties (actual unit composition and molecular weight) of the polymeric thermometers are summarized in Table 1.

The fluorescence responses of **1–3** were examined in 150 mM KCl solutions, which are equivalent to the cytoplasmic ionic environment of mammalian cells.[31] As shown in Fig. 3, the fluorescence spectra of **1–3** changed as the temperature varied from 25 to 45 °C, and the change in the fluorescence ratio at 580 to 515 nm (FI_{580}/FI_{515}, at which the fluorescence primarily originates from the DBThD-AA and BODIPY-AA units, respectively) was strongly correlated with the temperature. Among **1–3**, the cationic fluorescent polymeric thermometer **1** showed the most sensitive fluorescence response to the temperature variation (4.1% °C^{-1}, see Table 1). It is likely that the increase in the DBThD-AA unit content in
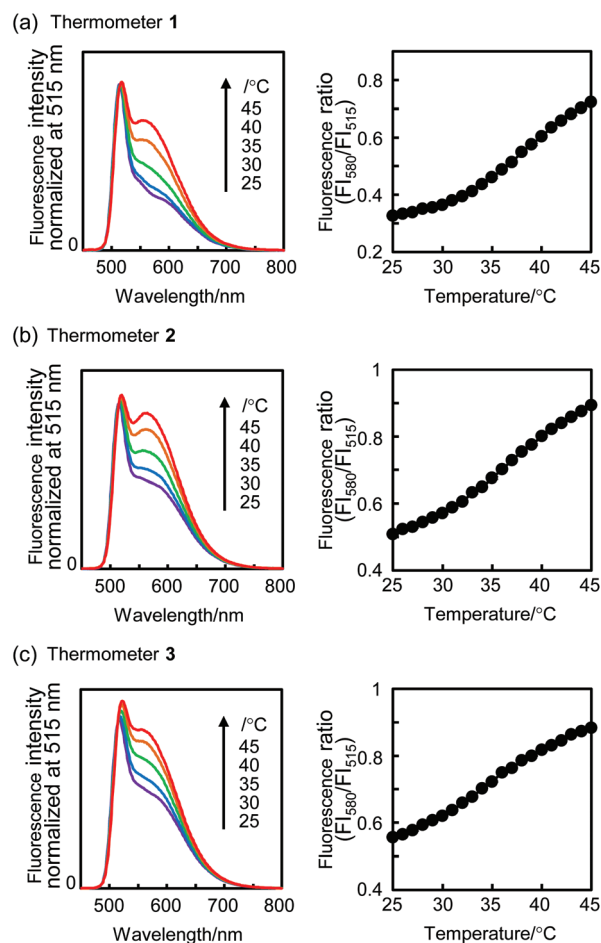

Fig. 3 Fluorescence responses of cationic fluorescent polymeric thermometers **1–3** in 150 mM KCl solution. Representative normalized fluorescence spectra (left) and fluorescence ratios at 580 to 515 nm (FI_{580}/FI_{515}, right) of (a) **1**, (b) **2** and (c) **3**. All samples (0.005 w/v%) were excited at 458 nm. The error bars for the fluorescence ratio representing the SD ($n = 3$) are too small to be visualized.

the polymeric thermometer causes its self-quenching.[32] Because it has the highest sensitivity, cationic fluorescent polymeric thermometer **1** was used in the subsequent intracellular thermometry of mammalian cells.

Functional independence of the cationic fluorescent polymeric thermometer 1

Fig. 4 shows the effects of the concentration of **1**, ionic strength and pH on the fluorescence signal (FI_{580}/FI_{515}) of **1**. As shown in Fig. 4, almost identical fluorescence response curves were obtained under different environmental conditions. The fluorescence response of **1** to temperature variation was independent of the concentration of **1**, the ionic strength in the range of 0.25–0.35 and the environmental pH between 6 and 9. This functional independence of the cationic fluorescent polymeric thermometer **1** is advantageous for accurate monitoring of intracellular temperature because these environmental conditions, especially pH, could be locally variable within living cells.[33]

Application of the cationic fluorescent polymeric thermometer 1 to non-adherent MOLT-4 cells

The cationic fluorescent polymeric thermometer **1** was introduced into non-adherent MOLT-4 cells using an experimental procedure previously established for a related, but non-ratiometric, fluorescent polymeric thermometer,[4a] *i.e.*, the cells were treated with 0.05 w/v% of **1** in a 5% glucose solution at 25 °C for 10 min. Fig. 5 summarizes the results obtained using MOLT-4 cells. The cationic fluorescent polymeric thermometer **1**
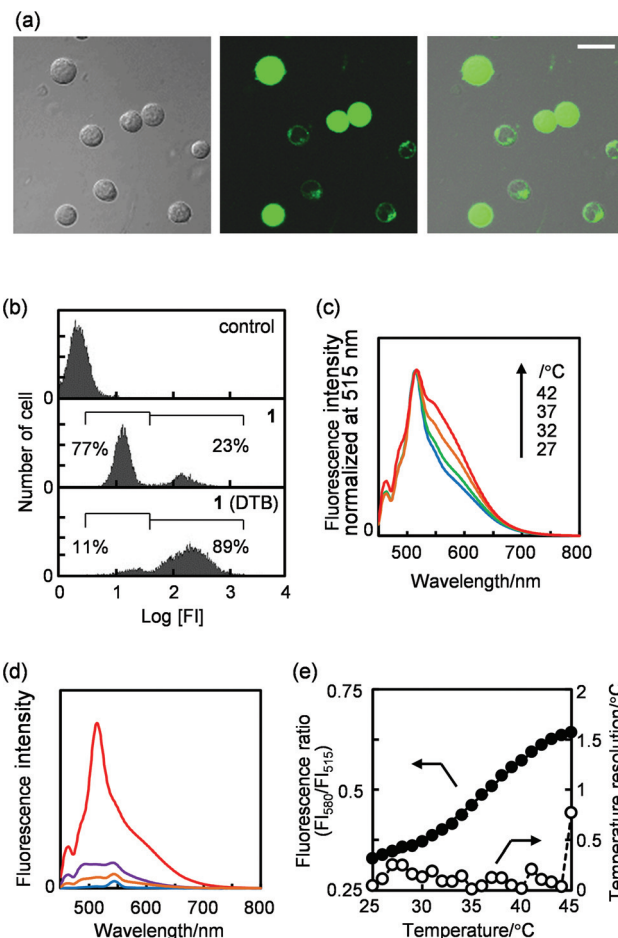

Fig. 5 Function of cationic fluorescent polymeric thermometer **1** in MOLT-4 cells. (a) Representative images of MOLT-4 cells treated with **1**. Differential interference contrast (DIC) image (left), confocal fluorescence image (middle) and the merged image (right). Scale bar represents 20 μm. (b) Histograms of fluorescence intensity (FI) in MOLT-4 cells treated without **1** (upper), with **1** (middle) and with **1** after double thymidine block (DTB) treatment (lower). The SDs (n = 3) for the percentages shown are 2.5% (middle) and 0.5% (lower). (c) Fluorescence spectra of **1** in MOLT-4 cells at 27, 32, 37 and 42 °C. The spectra are normalized at 515 nm. (d) Fluorescence spectra of MOLT-4 cells containing **1** (red), MOLT-4 cells (autofluorescence, purple), the supernatant of a suspension of MOLT-4 cells treated with **1** (orange) and PBS (blue) at 25 °C. The samples were excited at 458 nm. (e) Fluorescence response (closed, left axis) and temperature resolution (open, right axis). The error bars for the fluorescence response representing the SD (n = 3) are too small to be visualized.
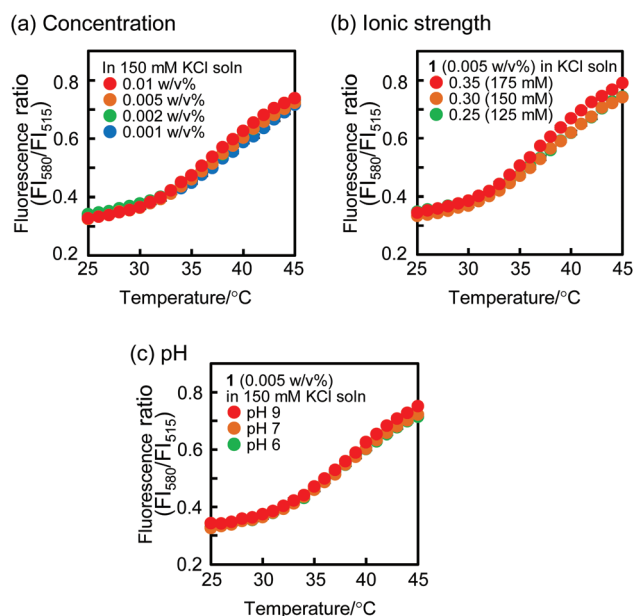

Fig. 4 Functional independence of **1**. Effects of (a) the concentration of **1**, (b) ionic strength and (c) pH on the fluorescence response (FI_{580}/FI_{515}) of **1** in KCl solutions. Samples were excited at 458 nm. The error bars representing the SD (n = 3) are too small to be visualized. HCl (0.1 mol l^{-1}) and KOH (1 mol l^{-1}) were used to adjust the pH.

was introduced into nearly all of the MOLT-4 cells (incorporation efficiency: 99.2 ± 1.1%) (Fig. 5a), although the fluorescence intensity varied among these cells, and some cell populations showed stronger fluorescence compared with the remaining cells. This variation in the amount of **1** incorporated into the cells was clearly revealed by flow cytometry analysis of the MOLT-4 cells treated with **1** (Fig. 5b, middle). One reason for the difference in the amount of **1** introduced into the MOLT-4 cells could be due to a difference in the phase of the cell cycle. When the cell cycle of the MOLT-4 cells was syn-

chronized to the G1/S phase *via* a double thymidine block,[30] the proportion of cells showing stronger fluorescence increased to 89% (Fig. 5b, bottom). The high incorporation efficiency in the G1/S phase is likely due to the decrease in the microviscosity of the plasma membrane and the corresponding increase in permeability.[34] The propidium iodide (PI) assay[35] indicated that nearly all of the MOLT-4 cells containing **1** were unstained with PI and, thus, were viable (fraction of live cells: 97.9 ± 1.7%).

Then, the fluorescence response of **1** to a temperature variation in the MOLT-4 cells was monitored using a spectrofluorometer with a mass of cells (*i.e.*, a cell suspension in a cuvette). The fluorescence spectra of MOLT-4 cells treated with **1** changed in response to the cellular temperature (Fig. 5c). The fluorescence signals observed in Fig. 5c originated predominantly from **1** introduced into the MOLT-4 cells (see Fig. 5d). Fig. 5e indicated the temperature-dependent fluorescence ratio at 580 to 515 nm (FI_{580}/FI_{515}) of **1** in the MOLT-4 cells (left axis). Through repeated measurements, the temperature resolution of **1** for the intracellular thermometry of MOLT-4 was determined to be 0.01–0.25 °C in the temperature range between 25 and 44 °C (Fig. 5e, right axis). This temperature resolution was comparable with those of the previously reported fluorescent thermometers [fluorescent polymeric thermometer (0.18–0.58 °C),[3] fluorescent nanogel thermometer (0.29–0.50 °C),[5] europium complex containing nanoparticles (1.0 °C),[7c] green fluorescent protein (1.2 °C),[9a] quantum dot/quantum rod complex (0.2 °C),[10] molecular beacon (0.2–0.7 °C),[11] gold nanocluster (0.3–0.5 °C)[12] and nanodiamond (0.044 °C)[13]].

Application of the cationic fluorescent polymeric thermometer 1 to adherent HEK293T cells

The thermometer **1** was applied to the intracellular thermometry of adherent HEK293T cells. As with the MOLT-4 cells, **1** was spontaneously introduced into HEK293T cells (Fig. 6a). No dead HEK293T cells were found in the PI assay. As shown in Fig. 6a, the amount of **1** introduced into the HEK293T cells varied. Nevertheless, fluorescence from thermometer **1** was observed in most HEK293T cells (incorporation efficiency: 92.9 ± 2.4%). Thermometer **1** diffused throughout the HEK293T cells, and the spatial resolution was diffraction limited (*ca.* 240 nm), which was equal to the maximum achieved by conventional fluorescent thermometers.[3,4,9] Our previous study revealed that an *N*-alkylacrylamide-based polymeric thermometer was delocalized in living cells indicating a homogeneous polarity.[4b] Thus, the fluorescence signal of **1** is considered to be sensitive only to the local temperature. The HEK293T cells that contained a considerable amount of **1** enabled us to measure the fluorescence spectra of **1** in the cells using a confocal microscope (Fig. 6b). As shown in Fig. 6b, thermometer **1** provided temperature-dependent fluorescence spectra, which were suitable for the ratiometric sensing of the intracellular temperature inside HEK293T cells. Although the fluorescence spectra exhibited moderate devi-
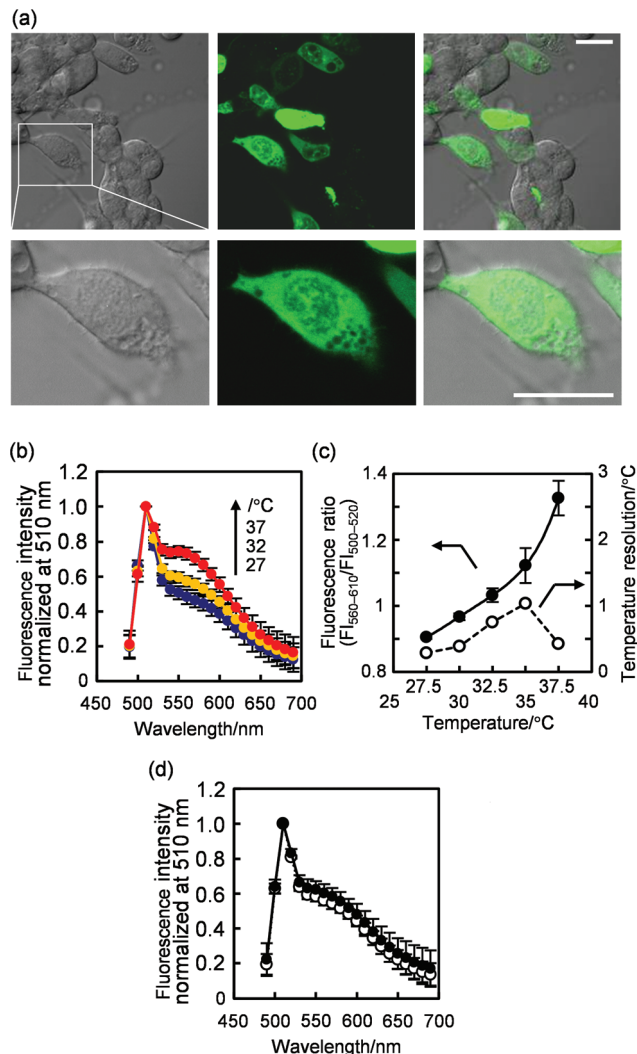

Fig. 6 Function of cationic fluorescent polymeric thermometer **1** in HEK293T cells. (a) Representative images of HEK293T treated with **1**. Differential interference contrast (DIC) image (left), confocal fluorescence image (middle) and the merged image (right). The region of interest, as indicated by the square in the left upper panel, is enlarged in the lower panels. When acquiring the fluorescence image, the excitation power was optimized for visualization of HEK293T cells containing a considerable amount of **1**. Scale bars represent 20 μm. (b) Averaged fluorescence spectra of **1** in a single HEK293T cell (*n* = 9, mean ± SD) at 27, 32 and 37 °C. (c) Fluorescence response (closed, left axis, *n* = 3, mean ± SD) and temperature resolution (open, right axis) of **1** in a HEK293T cell extract. $FI_{560-610}$ and $FI_{500-520}$ are the total fluorescence intensities between 560 and 610 and between 500 and 520, respectively. (d) Averaged fluorescence spectra of **1** in the nucleus (closed) and in the cytoplasm (open) in a single HEK293T cell (*n* = 9, mean ± SD) at 32 °C. The temperatures were of the culture medium. The spectra are normalized at 510 nm.

ations (see error bars), these deviations were due to cell-to-cell variation (*n* = 9) and not due to experimental error.

The temperature resolution was evaluated using a solution of **1** in a HEK293T cell extract.[3] Fig. 6c shows the change in the fluorescence ratio of 585 ± 25 nm to 510 ± 10 nm as the

temperature varied between 27.5 and 37.5 °C (left axis). The temperature resolution evaluated from the response curve was 0.29–1.0 °C in the studied temperature range. This temperature resolution of the thermometry when using a confocal microscope was lower than that (0.01–0.25 °C) when using a spectrofluorometer as described in the previous section. This lower temperature resolution was due to the difficulty in maintaining the temperature of the microscope stage (especially at high temperatures, see the large error bars in the fluorescence ratio at 35 and 37.5 °C).

In our previous studies, it was elucidated that the temperature of the nucleus is higher than that of the cytoplasm in COS7 cells.[3,4b] The temperature gap between the nucleus and the cytoplasm was also observed in the present fluorescence thermometry of HEK293T cells. As demonstrated in Fig. 6d, the averaged fluorescence intensity at approximately 585 nm (derived from DBThD-AA units) in the nucleus was higher than that in the cytoplasm, which corresponds to a temperature difference of ~1 °C.

Finally, we discuss the differences between the ratiometric fluorescence intensity measurements and the fluorescence lifetime measurements by comparing the functionality of **1** with that of our previously reported fluorescent polymeric thermometers. The former has clear advantages in terms of accessibility to measurement equipment and temporal resolution. In our intracellular thermometry experiments, a fluorescence ratio image could be collected within 1 s, whereas obtaining a fluorescence lifetime image requires 1 min to collect a sufficient number of photons. In closing, the new cationic fluorescent polymeric thermometer **1** possessed significantly improved practical utility for measuring the temperature inside cells. Intracellular thermometry of various cell lines, such as brown adipocytes, is ongoing using **1**, so that the intracellular temperature could be correlated with cellular functions. The wide distribution of **1** inside living cells will enable intracellular temperature mapping for the monitoring of the temperature at specific locations within living cells; this result will be reported in forthcoming biological research projects.

Acknowledgements

Notes and references

1 (a) K. M. McCabe and M. Hernandez, *Pediatr. Res.*, 2010, **67**, 469; (b) N. Inada and S. Uchiyama, *Imaging Med.*, 2013, **5**, 303.
2 (a) D. Jaque and F. Vetrone, *Nanoscale*, 2012, **4**, 4301; (b) C. D. S. Brites, P. P. Lima, N. J. O. Silva, A. Millán, V. S. Amaral, F. Palacio and L. D. Carlos, *Nanoscale*, 2012, **4**,

4799; (c) X.-d. Wang, O. S. Wolfbeis and R. J. Meier, *Chem. Soc. Rev.*, 2013, **42**, 7834.
3 K. Okabe, N. Inada, C. Gota, Y. Harada, T. Funatsu and S. Uchiyama, *Nat. Commun.*, 2012, **3**, 705.
4 (a) T. Tsuji, S. Yoshida, A. Yoshida and S. Uchiyama, *Anal. Chem.*, 2013, **85**, 9815; (b) T. Hayashi, N. Fukuda, S. Uchiyama and N. Inada, *PLoS One*, 2015, **10**(2), e0117677.
5 C. Gota, K. Okabe, T. Funatsu, Y. Harada and S. Uchiyama, *J. Am. Chem. Soc.*, 2009, **131**, 2766.
6 C. F. Chapman, Y. Liu, G. J. Sonek and B. J. Tromberg, *Photochem. Photobiol.*, 1995, **62**, 416.
7 (a) O. Zohar, M. Ikeda, H. Shinagawa, H. Inoue, H. Nakamura, D. Elbaum, D. L. Alkon and T. Yoshioka, *Biophys. J.*, 1998, **74**, 82; (b) K. Oyama, M. Takabayashi, Y. Takei, S. Arai, S. Takeoka, S. Ishiwata and M. Suzuki, *Lab Chip*, 2012, **12**, 1591; (c) Y. Takei, S. Arai, A. Murata, M. Takabayashi, K. Oyama, S. Ishiwata, S. Takeoka and M. Suzuki, *ACS Nano*, 2014, **8**, 198.
8 J.-M. Yang, H. Yang and L. Lin, *ACS Nano*, 2011, **5**, 5067.
9 (a) J. S. Donner, S. A. Thompson, M. P. Kreuzer, G. Baffou and R. Quidant, *Nano Lett.*, 2012, **12**, 2107; (b) J. S. Donner, S. A. Thompson, C. Alonso-Ortega, J. Morales, L. G. Rico, S. I. C. O. Santos and R. Quidant, *ACS Nano*, 2013, **7**, 8666.
10 A. E. Albers, E. M. Chan, P. M. McBride, C. M. Ajo-Franklin, B. E. Cohen and B. A. Helms, *J. Am. Chem. Soc.*, 2012, **134**, 9565.
11 G. Ke, C. Wang, Y. Ge, N. Zheng, Z. Zhu and C. J. Yang, *J. Am. Chem. Soc.*, 2012, **134**, 18908.
12 L. Shang, F. Stockmar, N. Azadfar and G. U. Nienhaus, *Angew. Chem., Int. Ed.*, 2013, **52**, 11154.
13 G. Kucsko, P. C. Maurer, N. Y. Yao, M. Kubo, H. J. Noh, P. K. Lo, H. Park and M. D. Lukin, *Nature*, 2013, **500**, 54.
14 S. Kiyonaka, T. Kajimoto, R. Sakaguchi, D. Shinmi, M. Omatsu-Kanbe, H. Matsuura, H. Imamura, T. Yoshizaki, I. Hamachi, T. Morii and Y. Mori, *Nat. Methods*, 2013, **10**, 1232.
15 C. Wang, R. Xu, W. Tian, X. Jiang, Z. Cui, M. Wang, H. Sun, K. Fang and N. Gu, *Cell Res.*, 2011, **21**, 1517.
16 (a) N. Inomata, M. Toda, M. Sato, A. Ishijima and T. Ono, *Appl. Phys. Lett.*, 2012, **100**, 154104; (b) M. K. Sato, M. Toda, N. Inomata, H. Maruyama, Y. Okamatsu-Ogura, F. Arai, T. Ono, A. Ishijima and Y. Inoue, *Biophys. J.*, 2014, **106**, 2458.
17 (a) L. Gao, L. Wang, C. Li, Y. Liu, H. Ke, C. Zhang and L. V. Wang, *J. Biomed. Opt.*, 2013, **18**, 026003; (b) L. Gao, C. Zhang, C. Li and L. V. Wang, *Appl. Phys. Lett.*, 2013, **102**, 193705.
18 (a) J. R. Lakowicz, in *Principles of Fluorescence Spectroscopy*, Springer, New York, 3rd edn, 2006, p. 624; (b) B. Valeur and M. N. Berberan-Santos, in *Molecular Fluorescence*, Wiley, Weinheim, 2nd edn, 2012, p. 411.
19 C. Gota, S. Uchiyama and T. Ohwada, *Analyst*, 2007, **132**, 121.

20 S. Uchiyama, K. Kimura, C. Gota, K. Okabe, K. Kawamoto, N. Inada, T. Yoshihara and S. Tobita, *Chem. – Eur. J.*, 2012, **18**, 9552.

21 F. L. Arbeloa, T. L. Arbeloa and I. L. Arbeloa, *J. Photochem. Photobiol., A*, 1999, **121**, 177.

22 C. Gota, S. Uchiyama, T. Yoshihara, S. Tobita and T. Ohwada, *J. Phys. Chem. B*, 2008, **112**, 2829.

23 H. G. Drexler, G. Gaedicke and J. Minowada, *Blut*, 1987, **54**, 79.

24 F. L. Graham, J. Smiley, W. C. Russell and R. Nairn, *J. Gen. Virol.*, 1977, **36**, 59.

25 Y. Maeda, T. Nakamura and I. Ikeda, *Macromolecules*, 2001, **34**, 1391.

26 H. Koutaka, J.-i. Kosuge, N. Fukasaku, T. Hirano, K. Kikuchi, Y. Urano, H. Kojima and T. Nagano, *Chem. Pharm. Bull.*, 2004, **52**, 700.

27 K. Suzuki, A. Kobayashi, S. Kaneko, K. Takehira, T. Yoshihara, H. Ishida, Y. Shiina, S. Oishi and S. Tobita, *Phys. Chem. Chem. Phys.*, 2009, **11**, 9850.

28 S. N. Baker, T. M. McCleskey and G. A. Baker, in *Ionic Liquids IIIB: Fundamentals, Progress, Challenges and Oppor-tunities: Transformations and Processes*, ACS Symposium Series 902, 2005, p. 171.

29 S. A. Latt and G. Stetten, *J. Histochem. Cytochem.*, 1976, **24**, 24.

30 J. Gong, F. Traganos and Z. Darzynkiewicz, *Cell Growth Differ.*, 1995, **6**, 1485.

31 H. Lodish, A. Berk, C. A. Kaiser, M. Krieger, A. Bretscher, H. Ploegh, A. Amon and M. P. Scott, in *Molecular Cell Biology*, Freeman, New York, 7th edn, 2013, p. 485.

32 In ref. 18*a*, pp. 69.

33 (*a*) G. R. Bright, G. W. Fisher, J. Rogowska and D. L. Taylor, *J. Cell Biol.*, 1987, **104**, 1019; (*b*) K. Ohtsuka, S. Sato, Y. Sato, K. Sota, S. Ohzawa, T. Matsuda, K. Takemoto, N. Takamune, B. Juskowiak, T. Nagai and S. Takenaka, *Chem. Commun.*, 2012, **48**, 4740.

34 (*a*) S. W. de Laat, P. T. van der Saag and M. Shinitzky, *Proc. Natl. Acad. Sci. U. S. A.*, 1977, **74**, 4458; (*b*) K. Niikura, K. Nambara, T. Okajima, Y. Matsuo and K. Ijiro, *Langmuir*, 2010, **26**, 9170.

35 K. H. Jones and J. A. Senft, *J. Histochem. Cytochem.*, 1985, **33**, 77.